MOLECULAR AND CELLULAR BIOLOGY, Aug. 1996, p. 4544–4554 Vol. 16, No. 8
0270-7306/96/$04.00+0

Precise Alignment of Sites Required for μ Enhancer Activation in B Cells

BARBARA S. NIKOLAJCZYK, BARBARA NELSEN, AND RANJAN SEN*

Rosenstiel Basic Medical Sciences Research Center and Department of Biology, Brandeis University, Waltham, Massachusetts 02254-9110

Received 29 November 1995/Returned for modification 9 January 1996/Accepted 3 May 1996

The lymphocyte-specific immunoglobulin μ heavy-chain gene intronic enhancer is regulated by multiple nuclear factors. The previously defined minimal enhancer containing the μA, μE3, and μB sites is transactivated by a combination of the ETS-domain proteins PU.1 and Ets-1 in nonlymphoid cells. The core GGAAs of the μA and μB sites are separated by 30 nucleotides, suggesting that ETS proteins bind to these sites from these same side of the DNA helix. We tested the necessity for appropriate spatial alignment of these elements by using mutated enhancers with altered spacings. A 4- or 10-bp insertion between μE3 and μB inactivated the μ enhancer in S194 plasma cells but did not affect in vitro binding of Ets-1, PU.1, or the μE3-binding protein TFE3, alone or in pairwise combinations. Circular permutation and phasing analyses demonstrated that PU.1 binding but not TFE3 or Ets-1 bends μ enhancer DNA toward the major groove. We propose that the requirement for precise spacing of the μA and μB elements is due in part to a directed DNA bend induced by PU.1.

A key molecular event in B-cell development is the activation of immunoglobulin (Ig) μ heavy-chain (μ) gene rearrangements in the earliest discernible B-cell precursor. Correlation of transcription activation with V(D)J recombination (1, 5) implicated the μ enhancer, located between the J_H and C_μ exons, as the probable regulatory target directing Ig heavy-chain gene recombination. The involvement of the μ enhancer in recombination and transcriptional activation was supported by the observation of sterile transcripts that initiated within the enhancer (31) and by the analysis of recombination substrates in cell lines (44) and transgenic mice (10). Furthermore, a role for this enhancer in regulating accessibility was suggested by the studies of Jenuwein et al. (23), who showed that a transgenic μ enhancer conferred access of bacterial RNA polymerases to adjacent DNA. Recently, genetic disruption of the μ enhancer in mice (8, 51) has directly demonstrated a role for this enhancer in Ig heavy-chain gene rearrangement.

The μ enhancer contains binding sites for multiple nuclear factors (32, 41). Three known elements, μA, μB, and octamer, bind proteins with restricted tissue distribution. In contrast, the majority of the factors that bind to the μE1 to μE5 sites in the μ enhancer can be detected in extracts made from B cells as well as nonlymphoid cells. These factors, including the E2A gene products, belong to the basic helix-loop-helix (bHLH) family of transcription factors (37) and have been implicated in both positive and negative regulation of the enhancer. For example, the μE5 motif that acts as a positive element in B cells (46) also interacts with a ubiquitous leucine zipper protein, ZEB, that has been proposed as a negative regulator of the enhancer (12). Secondly, in BxT somatic cell hybrids, where Ig heavy-chain expression is extinguished, one of the targets of repression is the μE4 element of the μ enhancer (52). Finally, a mutation of the E2A (bHLH) gene by homologous recombination results in a developmental block of B-cell differentiation at a very early stage (2, 61). Interestingly, the same phenotype is obtained by transgenic overexpression of Id-1, a protein known to heterodimerize with E2A gene products and prevent DNA binding by these proteins (54). Overall, these experiments indicate a critical role for bHLH gene products in lymphocyte differentiation.

In this array of factor-binding sites, mutation of a single element typically does not result in significant reduction of enhancer activity in plasma cells (32). This has been interpreted to indicate that there is substantial redundancy built into the enhancer. However, analysis of multiply mutated enhancers shows that elements that bind both the tissue-restricted and ubiquitous proteins are required for enhancer function. How these two types of proteins collaborate to generate a functional enhancer is, at present, unknown. To simplify further analysis of the μ enhancer, we have previously identified a minimal enhancer that contains no redundant motifs. The minimal enhancer contains the μA and μB elements that bind ETS-domain proteins (42), along with the μE3 element that binds several factors belonging to the bHLH-zip family (3, 4, 7, 16, 48, 49). The minimal enhancer is B-cell specific, and mutation of any one of the three sites significantly diminishes enhancer activity. Interestingly, the minimal enhancer is also a composite of tissue-restricted and ubiquitous protein-binding sites, suggesting that its analysis will provide insights into the mechanism of activation of the full μ enhancer.

Both μA and μB sites contain the consensus element (GGA) for binding members of the ETS-domain family of transcription factors (25). The ETS family member PU.1, a hematopoietic cell-specific protein, binds to the μB site and activates the μ enhancer weakly in nonlymphoid cells. Similarly, Ets-1, a more widely distributed protein, binds the μA site but alone does not activate the enhancer. In contrast, coexpression of Ets-1 and PU.1 in nonlymphoid cells results in synergistic activation of a reporter gene regulated by the minimal μ enhancer (42). Our current study addresses the mechanism underlying the transactivation of the μ enhancer by Ets-1 and PU.1.

Separation of the μA and μB sites by an integral number of helical turns of DNA suggested that the μA- and μB-binding

* Corresponding author. Phone: (617) 736-2454. Fax: (617) 736-2405. Electronic mail address: sen@binah.cc.brandeis.edu.

proteins interacted with the DNA from the same side of the helix. We tested whether alignment of the μA and μB sites was required for enhancer activity by inserting nucleotides to alter the distance between them. Although binding of one or more purified proteins to the enhancer was not weakened by the insertion mutations, alteration of the alignment between the *cis* elements inactivated the μ enhancer in fully differentiated B cells. Circular permutation and phasing analyses demonstrated that PU.1, but not TFE3 or Ets-1, bends DNA and therefore may contribute structurally to the μ enhancer multiprotein complex. Overall, our results suggest that a stereospecific multiprotein enhancer complex activates the Ig μ heavy-chain gene.

MATERIALS AND METHODS

Expression and purification of recombinant proteins. (i) His.PU. A 1.3-kb *Pvu*II-*Eco*RI fragment containing the full-length murine PU.1 cDNA was treated with the Klenow fragment of DNA polymerase plus deoxynucleoside triphosphates (dNTPs) and cloned into *Xho*I-digested, Klenow-treated pET14b plasmid (Novagen).

(ii) His.Ets. The ETS domain of Ets-1 was isolated from a pEV3S subclone (9a). The pEV3S subclone contained the ETS domain of Ets-1 amplified by PCR with the following primers: 5′-CCT GGG CCC GGG GCC CTG GCT GGC TAC AC-3′ (5′ primer) and 5′-CG GAG TCG ACG CTC AGG GGT GTA TCC CAG CAG-3′ (3′ primer). Ets-1/pEV3S was digested with *Bam*HI and *Xba*I, treated with Klenow fragment, and cloned into *Bam*HI-digested, Klenow-treated pET14b.

For protein expression, the plasmids were transformed into the BL21 bacterial strain. Protein production was induced with 0.4 mM isopropyl-β-D-thiogalactopyranoside (IPTG), and His-tagged proteins were purified without denaturing agents as specified by the manufacturer protocol (Novagen).

(iii) GST-TFE3 and GST-TFE3S. Bacterial expression vectors for GST-TFE3 and GST-TFE3S were kindly provided by Kathryn Calame, Columbia University, New York, N.Y.

Glutathione-*S*-transferase (GST) fusion proteins were purified as described previously (53). Expression of the recombinant protein was induced by the addition of IPTG to a final concentration of 0.4 mM for 3 to 5 h. After induction, the bacteria were pelleted and resuspended in NETN buffer (10 mM Tris-Cl [pH 8.0], 100 mM NaCl, 1 mM EDTA, 0.5% Nonidet P-40). Extracts were prepared by sonication (three pulses for 10 s each) at 0°C. The insoluble debris was removed by centrifugation, and the fusion protein was purified from the supernatant by adsorption to glutathione-agarose. Sonicated supernatant from 1 liter of bacteria was agitated with 1 ml of a 50% slurry of glutathione beads for 1 to 2 h at 4°C. The beads were washed three times with 25 to 30 ml cold NETN buffer. Adsorbed proteins were eluted with NETN buffer plus 5 mM reduced glutathione. Eluates (1 column volume) were collected and analyzed by sodium dodecyl sulfate-polyacrylamide gel electrophoresis, and the most highly concentrated fractions were pooled and dialyzed against buffer D (20 mM *N*-2-hydroxyethylpiperazine-*N*′-2-ethanesulfonic acid [HEPES; pH 7.9], 100 mM KCl, 0.2 mM EDTA, 0.5 mM dithiothreitol, 20% glycerol). Aliquots were frozen in liquid nitrogen and stored at −70°C.

EMSAs. Electrophoretic mobility shift assay (EMSA) probes were isolated as *Pst*I-*Bam*HI fragments from murine μ170 (bp 381 to 433 in the system of Ephrussi et al. [9]) cloned into Δ56CAT. After isolation from a 6% acrylamide gel, fragments were phosphorylated with polynucleotide kinase and [γ-^{32}P]ATP. EMSA reactions were carried out in a volume of 20 μl containing 10,000 cpm of probe, 2.5 μg of poly(dI-dC) · (dI-dC), and 2.0 μl of 10× lipage buffer (10× lipage is 100 mM Tris [pH 7.5], 0.5 M NaCl, 100 mM β-mercaptoethanol, 10 mM EDTA, and 40% glycerol). For EMSA with two recombinant proteins, both proteins were added to the reaction simultaneously. After a 10-min incubation at room temperature, the reaction products were electrophoresed through nondenaturing 4% polyacrylamide gels in 0.5× Tris-borate buffer (44 mM Tris borate, 44 mM boric acid, 2 mM EDTA). The gels were dried and visualized on DuPont film with an intensifying screen.

Plasmids. The +4, +10, and downstream +18 spacing mutations were made in the previously described M100 mutation (40), which introduces a *Sca*I site between μE3 and μB. For the +10 mutation, a *Spe*I linker (GGACTAGTCC) was ligated into *Sca*I-cut M100 DNA. The +4 mutation was generated by digesting the +10 mutation with *Spe*I followed by S1 nuclease treatment and religation. For the +18 mutation, M100 was digested with *Bam*HI and treated with Klenow fragment to produce blunt ends and then the *Spe*I linker was ligated into this site. The *Bam*HI introduced by site-specific mutagenesis of the core 1 (24) site lies 3′ of μB. All spacing mutations were generated in the context of the 700-bp *Xba*I-*Eco*RI fragment of the μ enhancer.

For transfection analyses, $\mu(70)_2$ plasmids were generated from the mutated enhancers by isolating the *Alu*I-*Alu*I fragment encompassing nucleotides 385 to 455 (numbering according to the system of Ephrussi et al. [9]) and cloning into the vector Δ56 fos CAT (15), which was cut with *Sal*I and treated with Klenow fragment.

For the μ170 plasmids, the *Hin*fI-*Dde*I enhancer fragments (residues 346 to 518 [9]) containing the mutations were treated with Klenow fragment and cloned into pBluescript SK+ cut with *Hinc*II. *Hin*dIII-*Xho*I fragments isolated from these clones were then ligated into Δ56 fos CAT cut with *Hin*dIII and *Sal*I. The orientation of the μ170 fragments is such that the 5′ *Hin*fI end of the enhancer is adjacent to the minimal *fos* promoter. All plasmids were purified with Qiagen 100 preparative columns and sequenced to confirm the presence of mutations and the orientations. The orientations of the μ70 dimers are as previously described by Nelsen et al. (42).

Murine S194 plasma cells were transfected with 5 μg of plasmid by the DEAE-dextran method as previously described (17) and harvested 42 to 48 hs posttransfection. Protein (5 to 10 μg) was analyzed in chloramphenicol acetyltransferase (CAT) assays as previously described (39), and the results were quantitated by phosphorimager analysis.

DNA-bending analysis. All bend angles were estimated from equations cited by Thompson and Landy (56) as modified by Kerppola and Curran (26). The position of the center of the DNA bend in circular permutation analysis was determined as a function of distance (in base pairs) from the end of the probe to the center of the μB GGAA by the method of Fisher et al. (11). Identical results for the DNA bend center were obtained relative to the center of the μE3 CATGTG core-binding site.

For circular permutation analysis, the *Pst*I-*Bam*HI Klenow-treated μ enhancer fragment (bp 381 to 433) was cloned into the Klenow-treated *Sal*I site of the pBend vector (29). Fragments were excised with *Mlu*I, *Spe*I, *Eco*RV, *Nru*I, or *Bam*HI, dephosphorylated, and ^{32}P labeled as described above for EMSA. Alternatively, a simian virus 40 (SV40).PU oligonucleotide (GAT CCC TCT GAA AGA GGA ACT TGG) was cloned into pBend and circular permutation fragments were excised with *Mlu*I, *Spe*I, *Eco*RV, *Nru*I, or *Rsa*I. EMSA analysis was performed as described above. The DNA flexure angle was calculated by using the equation $\mu_M/\mu_E = \cos(\alpha/2)$, in which μ_M is the mobility of the protein-DNA complex with the bend at the middle and μ_E is the mobility of the protein-DNA complex with the bend at the end. μ_M was determined from the *Eco*RV fragment for PU.1 or the *Nru*I fragment for TFE3S/USF. μ_E was determined from the *Bam*HI fragment for all proteins binding the μ enhancer, but the *Mlu*I fragments represented μ_E for the SV40.PU series. A standard curve was generated by measuring mobilities of fragments containing two to seven A tracts located either in the middle (μ_M) or at the end (μ_E) of the DNA fragment. The μ_M/μ_E ratio was plotted as a function of the poly(A)-tract-induced angle to derive the standard curve. Calculated values agreed well with values obtained from the standard curve. A coefficient, *k*, introduced by Kerppola and Curran (26) to account for gel and fragment size variables, was also calculated from these standard poly(A)-tract fragments by using the equation $\mu_M/\mu_E = \cos(k\alpha/2)$. For this calculation, it was assumed that each poly(A) tract bent the DNA to an 18° angle (56) such that for the fragment with two poly(A) tracts, $\alpha = 36°$, etc. The coefficient *k* (0.67) was used for quantitation of phasing analyses.

Probes for phasing analysis contained the *Pvu*II-*Bam*HI (bp 385 to 433) μ enhancer fragment, which was treated with Klenow or mung bean nuclease prior to ligation with the vector. Vectors were derived from pTK401-26 or pTK401-28 (26, 27) after excision of the AP-1 site with *Xba*I and *Sal*I and subsequent treatment with Klenow fragment and deoxynucleotides. Various combinations of fragments and vectors resulted in constructs containing 29, 34, 36, 39, or 41 bp between the centers of the μB site (between the C and A of the sequence 5′-TTCCCCAAA-3′) and the minor-groove bending A tracts. This distance was designated the spacer; spacer length differed depending on the protein-binding site, with μB spacers being the shortest and μA spacers being the longest.

Phasing analysis was quantitated from the best cosine curve fit to the EMSA phasing data. EMSA data were first expressed as complex mobility/mean mobility for all five phasing complexes and then plotted as a function of the number of base pairs between the middle of the protein-binding site and the middle of the 3′ phased A tracts by using KaleidaGraph. The fit of the cosine curve to the datum points was statistically significant (chi-square values, <0.005; *R* values, >0.98). The horizontal phase shift was subtracted from the spacer length to center the function near the *y* axis. This adjustment allowed determination of bend direction as described in Results. The amplitude of the cosine function is equal to the phasing amplitude, A_{PH}. A_{PH} used in conjunction with coefficient *k* and a standard bend angle (α_{std}) of 54° (for the three phased A tracts in the fragment) defines the circular permutation angle (α_{CP}) from the equation

$$\tan(k\alpha_{CP}/2) = \frac{(A_{PH}/2)}{\tan(k\alpha_{std}/2)}$$

RESULTS

Our previous analysis suggested that the μA and μB sites are essential for activation of the murine μ heavy-chain gene enhancer (42). Examination of the corresponding regions of the Ig heavy-chain locus from other mammalian species showed

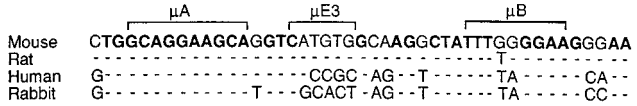

FIG. 1. Comparison of mammalian μ enhancer sequences. The human, rat, and rabbit enhancer sequences were obtained from Hayday et al. (20), Bruggemann et al. (6), and Mage et al. (35), respectively. μA, μE3, and μB sites of the murine enhancer are indicated by brackets above the sequence. Residues of the rat, human, and rabbit sequences that are identical to the murine sequence are indicated by dashes, and sequence differences shown as the altered base. Residues that are common to all sequences are shown in boldface type in the murine sequence.

that both μA and μB sites were highly conserved (10-of-10-nucleotide identity at μA and 7-of-9-nucleotide identity at μB [Fig. 1]). The nonconserved nucleotides in μB are not critical for activation of the enhancer, as previously demonstrated (40). Mutation of the μA or μB elements abolishes the activity of the minimal enhancer, but residual activity of the μE3 site mutation suggests that this site contributes to enhancer activation quantitatively. Interestingly, the spacing between the μA and μB motifs is evolutionarily conserved; however, we found that the μE3 site defined in the murine enhancer was absent in the human and rabbit enhancers (Fig. 1). Preservation of μA-μB spacing even in the absence of a recognizable E box suggested that correct spatial orientation of these two sites was critical for enhancer function.

Effect of insertion mutations on μ enhancer-protein binding. To test the hypothesis that the organization of the μA and μB sites and their cognate transcriptional activators was critical for enhancer activity in B cells, we constructed mutated μ enhancers with either 4 or 10 bp inserted between the μE3 and μB sites (Fig. 2A) and tested these mutations in DNA-binding and functional assays. To facilitate DNA manipulations, insertions were made in the M100 μ enhancer mutation, in which the AGG between μE3 and μB is changed to GTA to form a *Sca*I restriction endonuclease site. The M100 mutation does not affect μ enhancer activation in B cells (40), indicating that these changes do not alter functionally important sequences. Insertion of 4 or 10 bp rotates the μB site approximately 145° or 350°, respectively, relative to the μA or μE3 sites, assuming a DNA helical periodicity of 10.5 bp.

To eliminate the possibility that insertion of nucleotides between μE3 and μB interferes with known protein-μ enhancer interactions, we analyzed the binding of recombinant Ets-1, PU.1, or the prototypic bHLH-zip protein, TFE3, to the mutant enhancer sequences by EMSA. Full-length Ets-1 contains two inhibitory domains, positioned immediately 5′ or 3′ to the ETS domain, that interfere with DNA-binding activity (18, 33, 43, 58); therefore, the DNA-binding ETS domain of Ets-1 [amino acids 325 to 426; referred to as ETS(Ets-1)] was used in these assays in lieu of the full-length protein. Increasing amounts of ETS(Ets-1) were added to DNA probes derived from the M100, +4, or +10 mutated μ enhancers (Fig. 2B). No difference in complex formation (E) was seen with these three probes (Fig. 2B, M100 [lanes 1 to 4], +4 [lanes 5 to 8], and +10 [lanes 9 to 12]). Similarly, addition of increasing amounts of TFE3 to M100 or the insertion mutations resulted in similar patterns of protein-DNA complexes with any of the three fragments (Fig. 2C; compare lanes 1 to 4 with lanes 5 to 8 and lanes 9 to 12). Mobility shift assays of PU.1 with μ enhancer DNA resulted in a more complex pattern. At low protein concentrations, PU.1 formed a single major nucleoprotein complex with the M100 probe (P; Fig. 2D, lane 1) whereas additional, more slowly migrating complexes appeared at higher protein concentrations (2P; lanes 2 to 4). The major complex represents PU.1 bound to the μB site, as confirmed by its absence when a μB^- probe was used in these assays (data not shown), whereas the more slowly migrating complex probably represents occupancy of both μA and μB sites by PU.1. The proposed composition of the second complex (2P) was confirmed by EMSA results with a μA mutated enhancer fragment (μA^-), which formed only the PU.1-μB complex even at high PU.1 concentrations (lanes 13 to 16). DNase I footprint analysis confirmed that PU.1 was bound to both μB and μA sites at high protein concentrations (data not shown). We hypothesize that the main recognition of the μ enhancer by PU.1 occurs via the μB element, and μB binding is followed by recruitment of another molecule of PU.1 to the μA site. A similar pattern of PU.1 binding was observed with the +4 and +10 nucleotide insertion mutation enhancers in both EMSA (Fig. 2D, lanes 5 to 12) and DNase I footprint analyses (data not shown). We conclude that the spacing mutations do not affect the binding of Ets-1, TFE3, or PU.1 to μ enhancer DNA.

Effect of insertion mutations on $(\mu 70)_2$ and μ170 enhancer activation. To determine the effect of the insertion mutations on μ enhancer function, we tested the mutants for activity in S194 plasma cells by transient-transfection analyses (Fig. 3). As noted previously (42), the minimal enhancer, μ70, was analyzed as a dimer to amplify small differences. The M100 $(\mu 70)_2$-containing reporter plasmid was as active as the wild-type $\mu(70)_2$ reporter in S194 cells (data not shown). Insertion of 4 or 10 nucleotides between the μE3 and μB sites dramatically decreased the activity of M100 $(\mu 70)_2$ derivatives (labeled M100 [+4] and M100 [+10]) to 13 or 14% of M100 activation, respectively (Fig. 3A). To rule out the possibility that the observed results were due to alteration of the spacing between the two μ70 fragments, we analyzed a minimal enhancer that contained 18 nucleotides introduced 3′ of the μB site (M100 [+18]). This enhancer was significantly more active than either the +4 or +10 enhancers, supporting the view that alteration of spacing between μ70 monomers or between the enhancer and promoter was not detrimental to enhancer activity.

Because the minimal enhancer is critically dependent on the integrity of all three motifs, the M100 $(\mu 70)_2$ dimer experiments did not distinguish whether the observed effects were due to disruption of μA/μB-binding protein interactions or to disruption of μE3/μB-binding protein interactions. In a larger enhancer fragment, such as the μ170 which contains μE1, E2, E3, and E5 motifs, enhancer activity is much less dependent on the μE3 element. However, mutation of either μA or μB elements in this context abolishes enhancer function (42). We reasoned that if the spacing mutations affected only μE3/μB-binding protein interactions, the effect of these mutations in the context of μ170 should be similar to that of a $\mu E3^-$ mutation. Alternatively, if μA/μB interactions were affected, the spacing mutant activity should resemble the activity of μA^- or μB^- enhancers. We tested the effects of insertions in the context of the μ170 enhancer by transient transfection of S194 cells (Fig. 3B). Addition of 4 bp between μE3 and μB decreased enhancer activity by 75%, and insertion of 10 bp resulted in a 90% reduction in transcriptional activation. The activity of the spacing mutants was therefore comparable to that of the μA^- and μB^- mutant μ170 enhancers. In contrast, the μE3 mutation did not reduce μ170-activated CAT expression significantly. Because the spacing mutations were functionally similar to the μA^- or μB^- mutations and unlike the $\mu E3^-$ mutation, we propose that the observed effects are due to disruption of appropriate spacing between the μA and μB

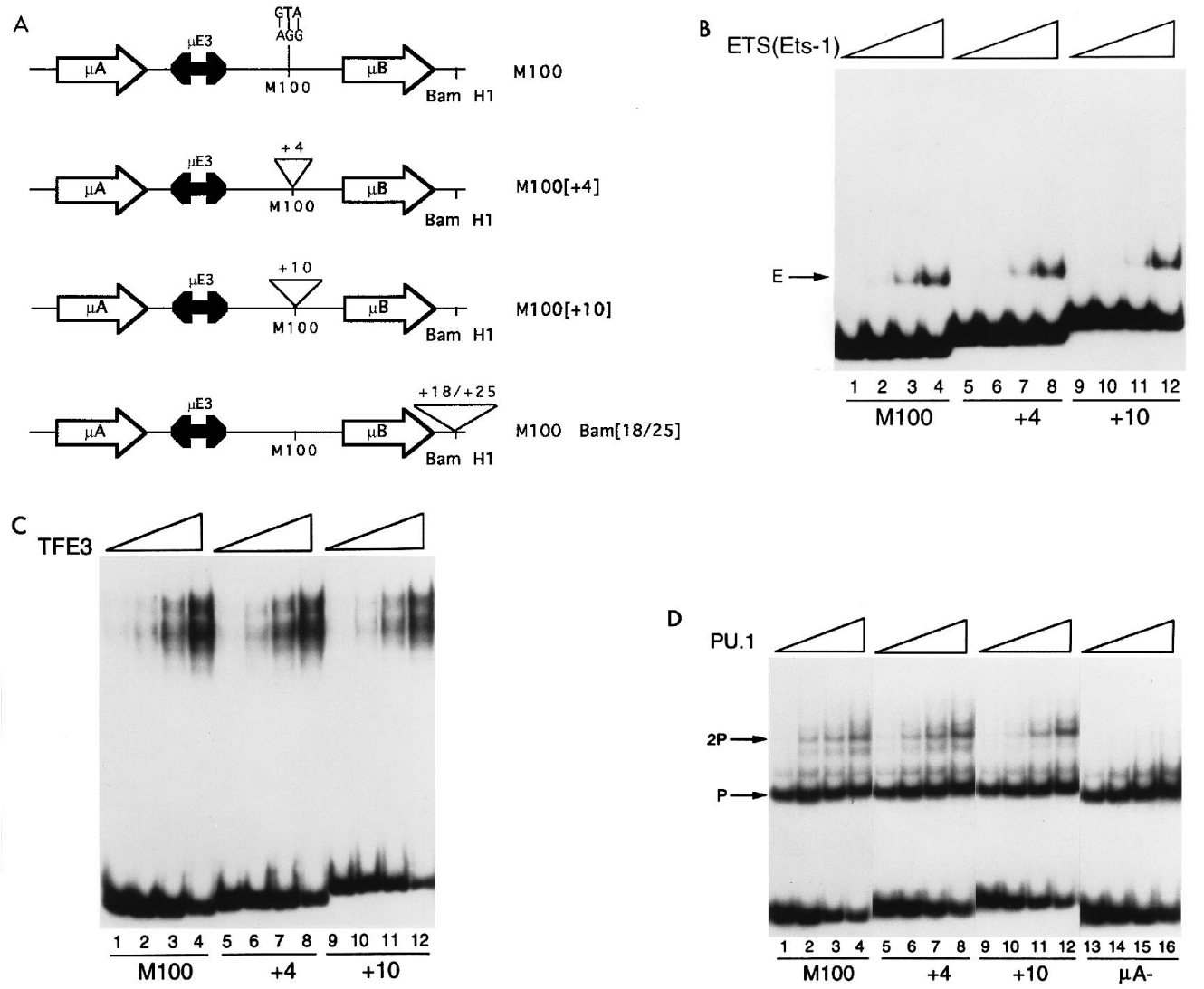

FIG. 2. Binding analysis of mutant enhancers that alter the distance between μB and the 5′ μA or μE3 elements. (A) μ enhancer spacing mutants were made in the context of the functionally active M100 mutation as described in Materials and Methods. The μA and μB sites are shown as single-headed arrows, and the intervening μE3 element is shown as a double-headed arrow to indicate its partially palindromic nature. As a control, *Spe*I linkers were also used to introduce the same nucleotides 3′ of the μA/μE3/μB functional region at a unique *Bam*HI site engineered into the first core homology. μ70 constructs contained a single linker (18 additional nucleotides) at the *Bam*HI site (M100 Bam[+18]), whereas μ170 constructs contained two linkers and (25 additional nucleotides; M100 Bam[+25]) at this site. Four (GGCC) or 10 (GGACTAGTCC) nucleotides were inserted between μE3 and μB as indicated. (B to D) EMSA analysis of protein binding to the spacing mutant enhancers. Increasing amounts of ETS-domain proteins or TFE3 were incubated with probes derived from M100 or mutant enhancers as indicated, followed by nondenaturing gel electrophoresis. Proteins used were the ETS domain of Ets-1, ETS(Ets-1) (B), the μE3-binding protein TFE3 (C), and PU.1 (D). The proposed single- and double-occupancy PU.1 complexes are indicated as P and 2P, respectively. μA^- refers to a probe containing a mutation in the μA element.

elements. We conclude that μ enhancer activity depends upon strict alignment of the μA and μB elements.

Binding of multiple proteins to the μ enhancer is not affected by the insertion mutations. The EMSA analyses shown in Fig. 2 indicated that binding of individual enhancer proteins is not affected by the spacing alterations. One mechanism by which insertion mutations may decrease μ enhancer activation is by affecting the formation of an appropriate multiprotein complex on the DNA. To examine potential perturbations in the formation of such a complex, we tested simultaneous binding of PU.1, Ets-1, and TFE3 in pairwise combinations (Fig. 4). Incubation of constant amounts of μA-binding ETS(Ets-1) with increasing amounts of μB-binding PU.1 demonstrated that the M100, +4, and +10 insertion mutants bound these proteins with indistinguishable affinities (Fig. 4A, compare M100 [lanes 1 to 4], +4 [lanes 5 to 8], and +10 [lanes 9 to 12]). The complex representing the PU.1/ETS(Ets-1) double occupancy (P/E) was seen at lower concentrations of PU.1 compared with the PU.1 double-occupancy band (2P). These results show that Ets-1 binding to the PU.1-occupied μ enhancer is preferred over binding of a second molecule of PU.1 to the μA site. Similar results were obtained in experiments with constant amounts of PU.1 and increasing concentrations of ETS(Ets-1) or full-length Ets-1 (data not shown). EMSA with full length Ets-1 and PU.1 also showed no differences in ETS protein binding to the M100 or spacing mutants (data not shown). Overall, simultaneous binding of PU.1 and Ets-1 was not affected by the functionally inactive +4- or +10-bp enhancer mutants.

To determine whether the insertions affected simultaneous

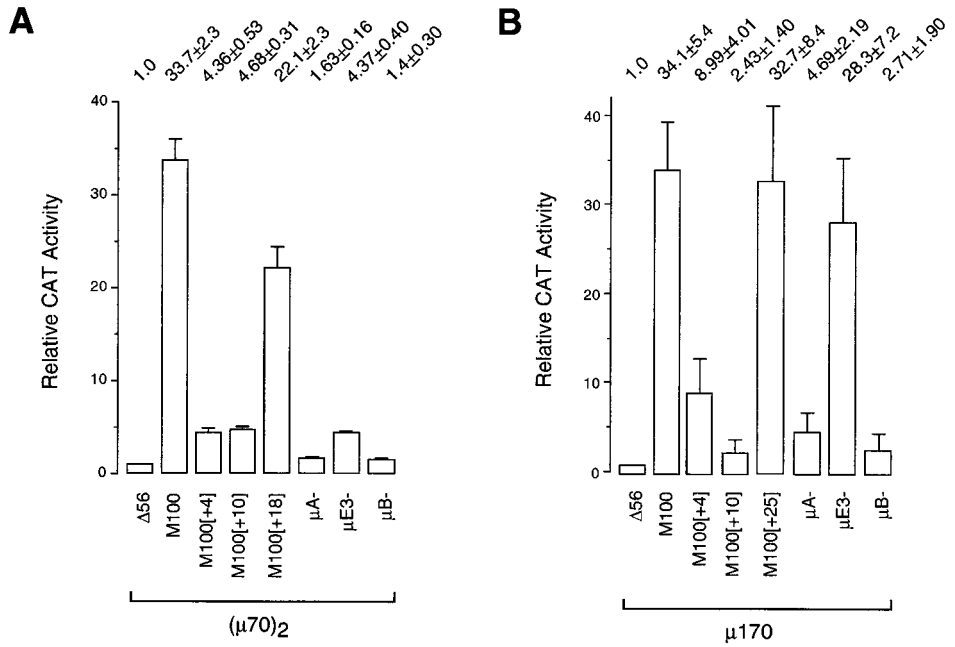

FIG. 3. Functional analysis of spacing-mutant μ enhancer constructs. M100 and spacing mutants were analyzed in the context of the μ70 minimal enhancer (A), or the larger μ170 enhancer (B) by transient transfections into S194 plasmacytoma cells. Relative chloramphenicol acetyltransferase activity shown on the *y* axis is the activity of reporter plasmids normalized to an enhancerless construct. M100 and spacing-mutant constructs are defined in Fig. 2A, and μA$^-$, μE3$^-$, and μB$^-$ mutants are from Nelsen et al. (42). Data presented are the mean of at least two transfections carried out in duplicate; error bars represent the range of values obtained in these experiments. Numerical values for the activity and range are shown above each graph.

binding of PU.1 and TFE3, we used a splice variant of TFE3 (TFE3S) (47) and PU.1 in EMSA. TFE3S retains the DNA-binding properties of TFE3 but results in a clearer, more easily interpreted pattern in EMSA. In these experiments, the amount of TFE3S was held constant while the concentration of PU.1 was increased. Consistent with the previous analyses of full-length TFE3 (Fig. 2C), the binding of TFE3S alone to the M100, +4, or +10 mutations was unchanged (Fig. 4B, lane 1, 6, and 11). TFE3S plus low concentrations of PU.1 formed one novel slowly migrating complex (P/T, lanes 2 and 3). At higher concentrations of PU.1, an additional complex, 2P/T, was formed (lanes 4 and 5). We hypothesize that the initial complex (P/T) represents PU.1 and TFE3S binding to the μB and μE3 sites, respectively; the most slowly migrating complex, 2P/T, represents PU.1 occupying both μA and μB in addition to TFE3S binding μE3. Similar patterns of complexes were generated on the +4 and +10 spacing mutations (+4 [lanes 6 to 10], +10 [lanes 11 to 15]). Interestingly, the initial (P/T) complex formed by PU.1 and TFE3S on the +4 enhancer DNA migrated faster than the P/T complexes formed on either the M100 or +10 enhancers. This difference was not seen in complexes containing TFE3S alone. We hypothesize that this altered mobility may be due to differences in DNA conformation induced by the binding of TFE3 and PU.1. TFE3 has been proposed to bend DNA (11, 48), but the DNA-bending properties of PU.1 are unknown. Because the TFE3-binding site in the +4 mutant is rotated with respect to the μB site by half a helical turn compared with both the M100 and +10 mutants, we suggest that the bends induced by each protein may neutralize each other and thereby result in the observed differences in electrophoretic migration. We did not examine Ets-1/TFE3 pairwise interactions, because the spacing mutants do not change the relative configuration of the μA and μE3 sites. Overall, both single and multiple protein-DNA binding assays demonstrated no significant difference in binding of Ets-1, TFE3, and/or PU.1 on M100 versus the insertion mutant enhancers. Therefore, these binding analyses with purified proteins do not provide a simple mechanism for the inactivation of the enhancer by the +4 or +10 mutations.

μ enhancer DNA flexure is increased by protein binding. The DNA-bending model proposed as the basis for the differential migration of P/T complexes formed on the M100 and +4 mutants was further analyzed by two methods: circular permutation and phasing analyses. For circular permutation analysis, the minimal μ enhancer was inserted between tandemly repeated restriction sites of the pBend vector (29). Digestion of the resultant plasmid with various endonucleases yielded fragments of identical size, with the minimal enhancer located at different positions (Fig. 5A). Circular permutation analysis detects alterations in protein-DNA complex mobilities that reflect changes in end-to-end DNA distance resulting from (i) protein-induced DNA structural changes and (ii) the changing position of the protein-binding element within the probe. The shorter end-to-end distance of a DNA molecule bent at its center is detected by a retardation of that molecule (probe 3) compared with a DNA molecule bent at one end (probe 5). Circular permutation analysis of PU.1 binding to the minimal enhancer demonstrated PU.1-induced changes in DNA flexure (Fig. 5B, lanes 1 to 5). Calculation of the bend angle indicated that PU.1 binding the μB site bent enhancer DNA by approximately 48°. Similar analysis of TFE3S (Fig. 5B, lanes 6 to 10) demonstrated that this bHLH-zip protein bent the μ enhancer by 40°. Interestingly, a second bHLH-zip protein, USF, induced a 60° DNA bend when bound to the μE3 site, suggesting that the extent of DNA bending was not determined solely by the DNA sequence (data not shown).

To determine whether PU.1-induced increase in μ enhancer flexure is a property of the ETS domain of PU.1 specifically or

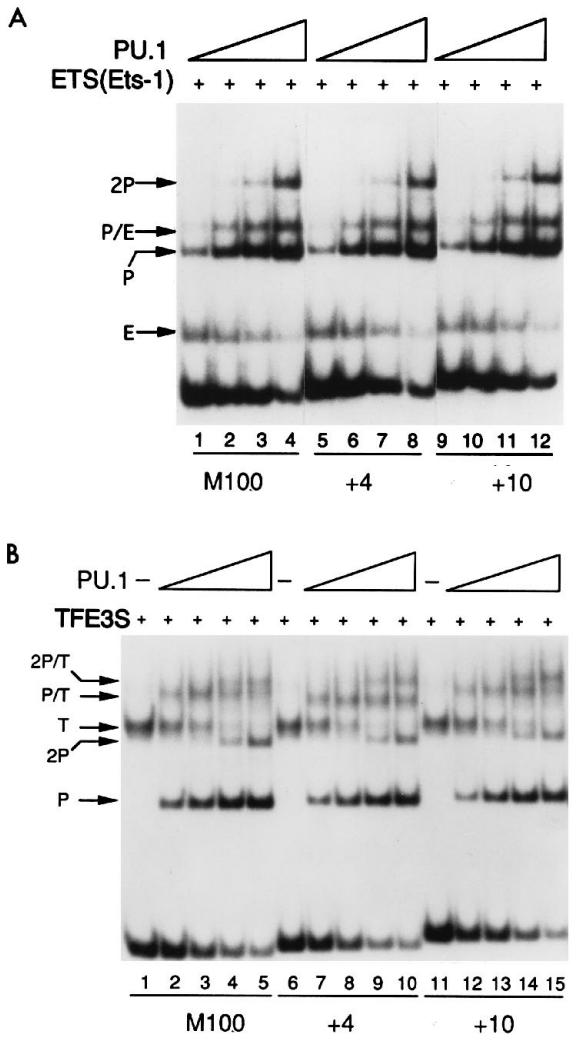

FIG. 4. Coordinate binding of two proteins to the μ enhancer spacing mutants. (A) Binding of the ETS domain of Ets-1, ETS(Ets-1), to the M100 (lanes 1 to 4), +4 (lanes 5 to 8), or +10 (lanes 9 to 12) mutant μ enhancers in the presence of increasing amounts of PU.1. ETS(Ets-1) bound to the μA site is designated complex E, with P and 2P indicating single and double occupancy, respectively, of the μB (and μA) sites by PU.1 as described in Fig. 2D. The ternary complex containing ETS(Ets-1), PU.1, and the μ enhancer is labeled P/E. (B) Binding of TFE3 (TFE3S) alone (lanes 1, 6, and 11) or with increasing amounts of PU.1 on the M100 (lanes 1 to 5), +4 (lanes 6 to 10), or +10 (lanes 11 to 15) mutant μ enhancers. Formation of single- and double-occupancy PU.1 complexes are designated P and 2P, respectively. The ternary PU.1-TFE3-μ enhancer complex is labeled P/T, and the quaternary 2PU.1-TFE3-μ enhancer complex is marked 2P/T. A splice variant of TFE3 which contains an intact bHLH-zip DNA-binding domain was used in these assays.

a general property of ETS domains, we repeated circular permutation analyses with the ETS domain of PU.1 [ETS(PU.1)] and ETS(Ets-1) (Fig. 5C). ETS(PU.1)-DNA complexes showed variable mobility with probes 1 to 5, as seen for the full-length PU.1 protein (Fig. 5C, lanes 1 to 5). However, all complexes with the ETS domain of Ets-1 migrated at approximately the same position, indicating that ETS(Ets-1) did not induce a conformational change in the DNA (Fig. 5C, lanes 6 to 10). To further confirm that PU.1-induced flexure change was not determined by the sequence of the μB element, we analyzed a different PU.1-binding site. Circular permutation analysis indicated that ETS(PU.1) bent DNA containing the SV40-PU.1 site to an apparent angle of 40° (data not shown), suggesting that bending was determined by the ETS domain of PU.1 rather than by the corresponding DNA element.

Circular permutation results were further analyzed to determine the center of the protein-induced DNA bend (Fig. 5D). Although this analysis cannot precisely localize the bend center, our results show that the PU.1-induced bend lies within the μB element (TTTGGGGAA). The TFE3-induced bend center is located a few nucleotides 5′ from the core CATGTG of the bHLH-zip binding site, μE3. We conclude that two of the three proteins that bind to the minimal μ enhancer induce conformational changes in the DNA.

Only PU.1 induces a directed bend in μ enhancer DNA. Although circular permutation analysis provides evidence for protein-induced DNA distortion, this assay more accurately reflects changes in DNA flexure that result from protein-DNA interactions. Alternatively, anomalous migrations in circular permutation assays may result from the nonglobular conformations of some DNA-binding proteins (26). To distinguish between DNA distortion and directed DNA bending, we performed phasing analysis. For phasing analysis, the μ enhancer fragment was cloned adjacent to three poly(A) tracts (26, 27). Each poly(A) tract confers an intrinsic DNA bend of 18°, for an overall 54° minor-groove-directed DNA bend. This bend serves as an internal standard against which protein-induced bending in the adjacent DNA fragment can be compared. The μ enhancer was cloned at five different distances from the poly(A) tracts to position it at various helical positions relative to the intrinsic minor-groove bend (Fig. 6A). Protein-induced bends directed toward the minor groove reinforce the intrinsic poly(A) tract bend when the protein-binding site is positioned at integral (*n*) helical turns from the poly(A) tracts. In contrast, major-groove bends reinforce the intrinsic bend when the protein-binding site is positioned on the opposite helical face (*n* + 5). If a DNA-binding protein induces only a change in flexure, the location of the binding site with respect to the poly(A) tracts does not affect DNA bending as assayed by nucleoprotein complex migration. EMSA analysis demonstrates bend reinforcement as decreased mobility of the DNA-protein complex.

We performed phasing analysis with ETS(PU.1), ETS(Ets-1), and TFE3S (Fig. 6B). Differences in protein-DNA complex mobility were apparent for ETS(PU.1) (lanes 1 to 5) but not ETS(Ets-1) (lanes 6 to 10) or TFE3S (lanes 11 to 15), indicating that only ETS(PU.1) induced a directed DNA bend. Results similar to ETS(PU.1) results were obtained for full-length PU.1 (data not shown). The PU.1-DNA complex was specifically inhibited by the μ enhancer phasing plasmid but not an AP-1 site-containing plasmid, indicating that PU.1 binds only μ enhancer elements in the phasing fragments (data not shown). Phasing analysis further allowed us to calculate the degree of ETS(PU.1)-induced DNA bending as described in Materials and Methods. The best-fit cosine curve for ETS(PU.1) (Fig. 7A) indicated a bend angle of 24°, after correction for the slight bend (1.0°) contributed by the DNA probe alone (Fig. 7B).

The direction of the ETS(PU.1)-induced DNA bend can also be ascertained from the phasing analysis once the center of the bend has been determined. Although circular permutation results indicated that the center of the ETS(PU.1)-induced flexure lies within the μB element, the precise bend center of this nonpalindromic site could not be determined. However, PU.1 binding to the μB site (5′-TTCCCCAAA-3′) induces a strong DNase I-hypersensitive site in the noncoding strand between the C and A residues, suggesting the presence of protein-induced distortion of the phosphodiester backbone

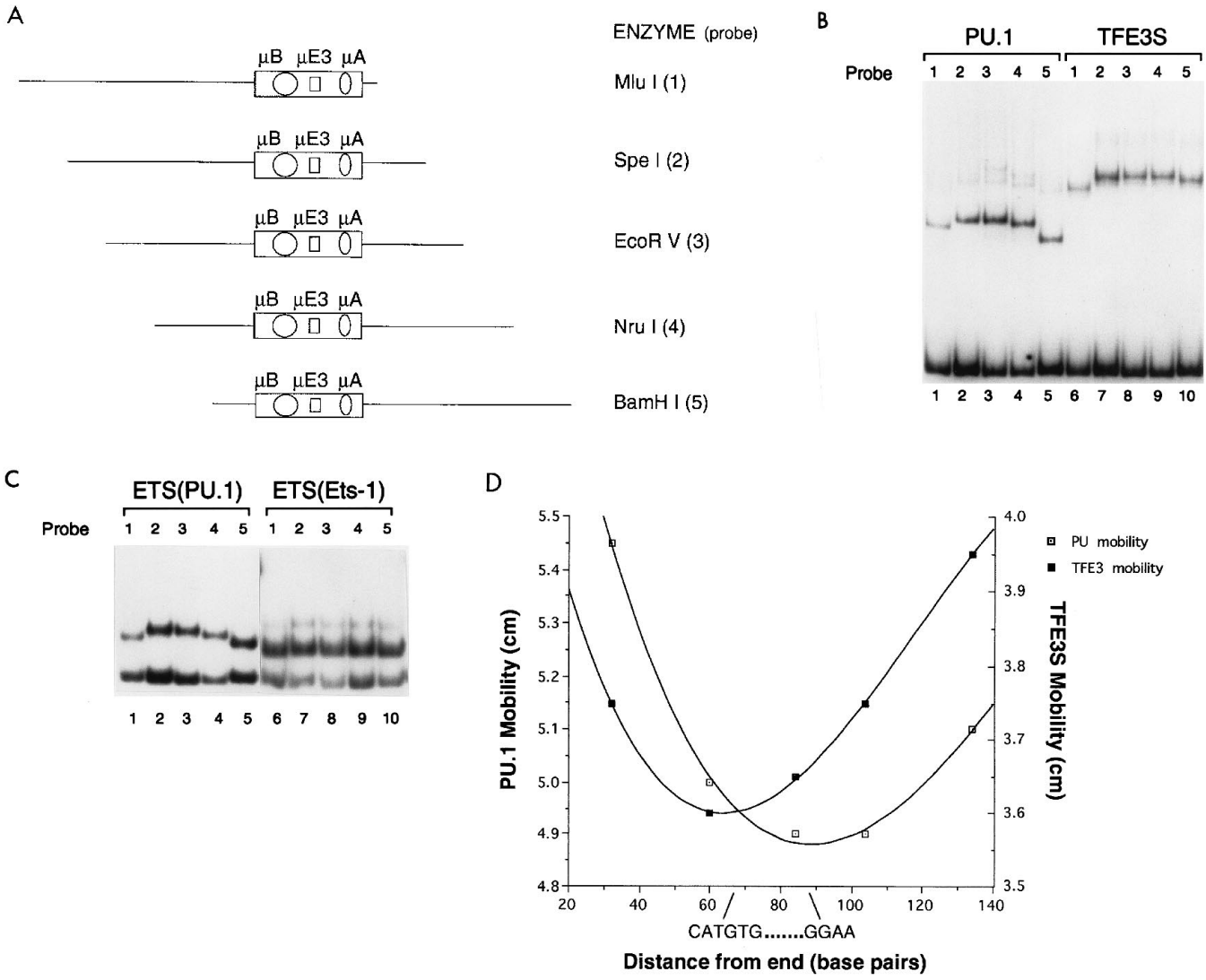

FIG. 5. Circular permutation of PU.1 binding to the μ enhancer. (A) Probes used in circular permutation assays. Fragments 1 to 5 containing μA, μE3, and μB were excised from the pBend vector with the designated enzymes. The μB site is located closest to the end of the fragment in probe 5 and closest to the middle of the fragment in probe 3. (B and C) Circular permutation analysis. Probes 1 to 5 were incubated with PU.1 (B), TFE3S (B), the ETS domain of PU.1 (C), or the ETS domain of Ets-1 (C) and assayed by electrophoresis through nondenaturing polyacrylamide gels. (D) Determination of the bend center for PU.1 and TFE3S. The mobilities of the protein-DNA complexes generated with the circular permutation probes were plotted as a function of the distance between the core GGAA of the μB and the 5′ end of each probe.

(45a). We approximated the hypersensitive site as the center of the PU.1-induced DNA bend and calculated the spacer lengths between μB and the poly(A) tract bend centers with reference to the position of this site. The ETS(PU.1)-induced DNA bend reinforced the poly(A) tract bend, resulting in the lowest-mobility nucleoprotein complex when the μB site was positioned 36 bp (3.4 helical turns) from the poly(A) tract. Because ETS(PU.1) reinforced the minor-groove-directed poly(A) tract bend when the μB element was on the opposite side of the DNA helix, we propose that ETS(PU.1) bends μ enhancer DNA toward the major groove.

Surprisingly, TFE3S did not induce a significant directed DNA bend (<1°) as measured by phasing analysis (Fig. 6B; cosine curve not shown), despite a greater than 40° change in flexure calculated from the circular permutation studies. This result conflicts with earlier reports (11, 48) of DNA bending by bHLH-zip proteins. We surmise that a significant proportion of the TFE3-induced conformational change may be attributed to a change in DNA flexure. Alternatively, it is possible that sequences flanking the bHLH-zip recognition element determine the extent of the protein-induced bend.

DISCUSSION

To facilitate mechanistic analysis of the lymphoid cell-specific immunoglobulin μ heavy-chain gene enhancer, we previously described a minimal enhancer that contains three sequence elements: μA, μE3, and μB (42). In this study, we demonstrate that appropriate spatial organization of the μA and μB sites is required for μ enhancer activity in B cells. In vitro analysis of purified Ets-1, TFE3, and PU.1 proteins that bind to the μA, μE3, and μB sites, respectively, showed that PU.1 but neither Ets-1 nor TFE3 induced a directed bend of approximately 24° in the enhancer DNA. We propose that the

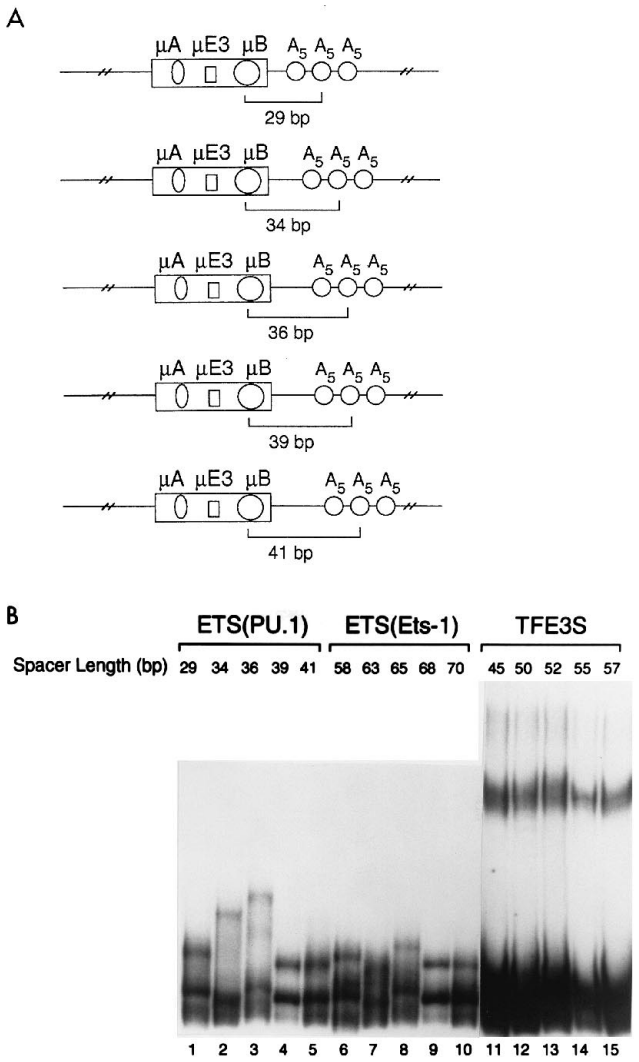

FIG. 6. Phasing analysis of μ enhancer-binding proteins. (A) DNA fragments used in the phasing analysis. The 55-bp μ enhancer fragment was inserted 5′ to three poly(A) tracts in previously described vectors (29, 30). Spacing between the μ enhancer and poly(A) tracts was varied to orient μ enhancer elements at different positions of the DNA helix with respect to the poly(A) tracts. The number of base pairs between the center of the core GGAA of μB and the center of the poly(A) tracts is indicated. This spacer length varied for μB, μA or μE3 elements as noted in panel B. (B) EMSA with DNA-phasing probes. Phasing probes were incubated with ETS(PU.1) (spacer length 29 to 41), ETS(Ets-1) (spacer length 58 to 70), or TFE3S (spacer length 45 to 57) and then analyzed by electrophoresis through 20-cm 4% acrylamide gels. The migration of each complex in EMSA reflects the net bend of the poly(A) tracts plus the protein-induced bend.

PU.1-induced bend in the DNA facilitates the formation of a functional multiprotein complex on the μ enhancer.

The importance of rotational alignment of *cis*-acting regulatory elements has been investigated in several systems. Most of these studies have focused on promoters and found that appropriate helical phasing is required for optimal activity, for example, the serine protease B gene, the *araBAD* operon, and the HLA-DR gene (19, 30, 57). In addition, helical periodicity has been observed for the interaction between the promoter and enhancer of simian virus 40 and human immunodeficiency virus (45, 55). A functional role for strict stereochemical relationship between motifs within an enhancer has been harder to demonstrate, perhaps because of the complex organization of enhancers. Several earlier studies have addressed this question as summarized below.

In the T-cell receptor (TCR) α-chain gene enhancer, a requirement for appropriate orientation of the Tα1 and Tα2 domains was suggested by altering the spacing between these elements. Functional assays indicated that for enhancer activation, Tα1 and Tα2 elements must be separated by more than 23 bp but less than 93 bp, without a strict dependence on the helical phasing between the two sites (22). A more recent analysis of the TCR α enhancer (14) showed that introduction of 4 nucleotides between the ATF/CREB and LEF/PEBP2/Ets-1 sites reduced enhancer activity; activity was restored by increasing the spacing to 10 nucleotides. These results indicate that optimal interaction between proteins bound at the ATF/CREB site and at one or more of the other sites requires appropriate helical phasing. Schanke and VanNess (50) showed that large changes in the positions of the κB and κE2 elements in the Ig κ light-chain enhancer resulted in loss of enhancer activity whereas small changes in their relative positions did not. These results indicated that the κ intron enhancer does not have strict spacing requirements.

Finally, a close juxtaposition of core-binding factor sites to other sites has been noted in the TCR β- and δ-chain gene enhancers (21, 60). Specifically, cooperative binding of Ets-1 and core-binding factor to the TCR β enhancer was shown to be independent of the distance between the two sites; however, the effects of moving the sites apart in transcriptional activation studies have not yet been determined. In contrast, transcriptional activity of the 30-bp δE3 element was abrogated by moving the binding sites for c-*myb* and core-binding factor by either 5 or 10 bp.

We found that introduction of 4 or 10 nucleotides between the μA/μE3 elements and the μB element essentially abolished the activity of both the μ70 minimal enhancer and the larger μ170 enhancer in B cells. Because mutation of the μE3 element did not affect μ170 enhancer activity, we propose that the insertion mutations inactivate the μ enhancer by disrupting interactions between ETS-domain proteins bound to the μA and μB sites. Such interactions may create a hybrid transactivation domain formed by ETS proteins bound to both sites, which could activate transcription by directly interacting with the basal transcription machinery. Alternatively, a third coactivator molecule may be recruited to the μ enhancer complex via interactions with appropriately positioned μA- and μB-binding proteins. Although synergistic interactions between *cis* elements is often reflected in cooperative DNA binding by the respective *trans*-acting factors, we did not detect cooperative binding of PU.1 and Ets-1 to μ enhancer DNA. Because the experiments were performed with bacterially expressed proteins, we cannot rule out the possibility that B-cell-specific posttranslational modifications are necessary to observe such effects or that PU.1 or Ets-1 functions with other ETS-domain genes expressed in B cells. Alternatively, our observations may reflect potential synergistic interactions between transcription factors at a level other than DNA binding.

A functional role for protein-induced DNA bends has been postulated for several transcription factors, such as catabolite activator protein (62), LEF-1 (13), retinoic acid receptors (34, 36), YY-1 (38) and the fos/jun protein family (26, 27). We found that of the three factors required to activate the minimal μ enhancer, only PU.1 induced a directed bend in the DNA as assayed by circular permutation and phasing analyses. It is interesting that binding of the related Ets-1 protein does not bend DNA, even though the DNA contacts previously defined for Ets-1 interaction with its cognate site (43) are very similar to those made by PU.1 at the μB site (45a). Our observations

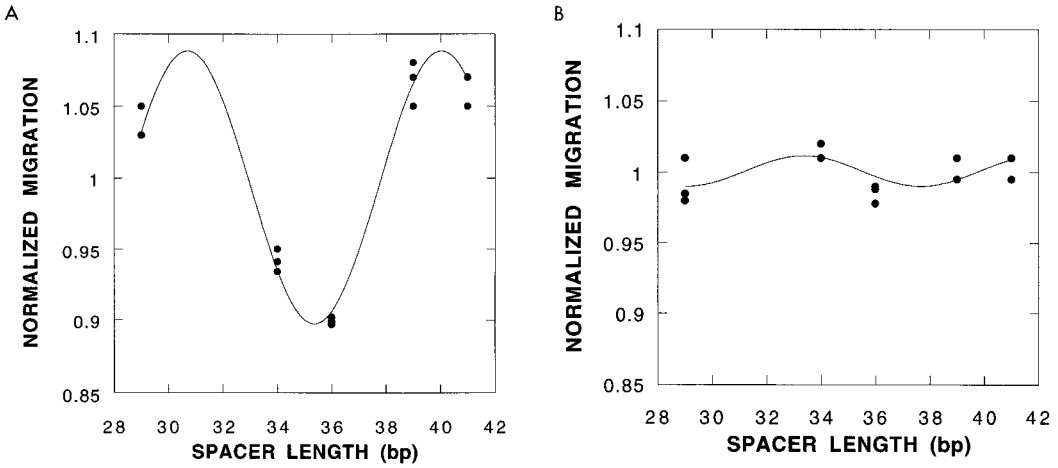

FIG. 7. Quantitation of directed DNA bend angles. (A) The migration of individual DNA-PU.1 complexes normalized to the average migration of all five complexes was plotted as a function of the distance between the center GGAA of μB and the center of the poly(A) tracts. Data from three experiments are shown, with some points being superimposed. The best-fit cosine function for the combined data was obtained by using KaliedaGraph. The resulting curve demonstrates a periodicity of about 10.5 bp, as expected for B-DNA. After subtraction of the horizontal phase shift, the maxima of the curve are at approximately 0 and 10 bp and the minimum of the curve lies at 5 bp. ETS(PU.1) therefore bends DNA toward the major groove. (B) The best-fit cosine function for the migration of DNA phasing probes alone ($n = 3$) demonstrates an insignificant (<1.0°) intrinsic bend in the μ enhancer DNA phasing probes.

suggest that ETS proteins may differ in their ability to induce DNA conformational changes. We speculate that DNA-bending properties may determine, in part, functional differences between ETS family members, as previously proposed for bZip family proteins (26–28). Because both ETS-1 and PU.1 proteins recognize their sites via the major groove, we suggest that PU.1-induced bending serves to align the two proteins bound to the μA and μB sites (Fig. 8).

Recently, Werner et al. (59) described a high-resolution structure of the ETS domain of Ets-1 bound to its recognition site. They found that DNA binding by ETS(Ets-1) induced a sharp kink in the DNA as a result of local compression of the major groove and widening of the minor groove. The distortion in the Ets-1/DNA complex is caused by intercalation of a tryptophan residue into the minor groove of the DNA between residues 6 and 7 of the Ets-1-binding site, 5′-TCGAGCCGG AAGTTCGA-3′. In our interpretation of the PU.1 phasing data, we approximated the center of the bend to the site of a strong PU.1-induced DNase I-hypersensitive site (on the noncoding strand) between residues 5 and 6 of the μB site, 5′-T ATTTGGGGAAGGGAA-3′. The close correspondence between the positions of the PU.1-induced hypersensitive site and Ets-1-induced DNA kinking suggests that PU.1 binding may similarly distort the DNA helix at this position. Furthermore, we have found that the three adenosine residues complementary to the three contiguous thymidines in the μB site score strongly in methylation interference assays (45a). Since the methyl group of methyl adenosines falls in the minor groove, these observations suggest that PU.1 is located over the minor groove in the vicinity of the PU.1-induced bend. Taken together with the phasing analysis that shows that the induced bend is towards the major groove, our observations are consistent with the DNA being bent away from the bound PU.1 protein. This facet of PU.1-DNA interaction is also consistent with the proposed structure of the Ets-1-DNA complex (59) and highlights the similarity of DNA recognition by these distantly related ETS-domain proteins. The proposed distortion of the DNA helix may facilitate interactions between the two proteins bound at the μA and μB sites of the μ enhancer.

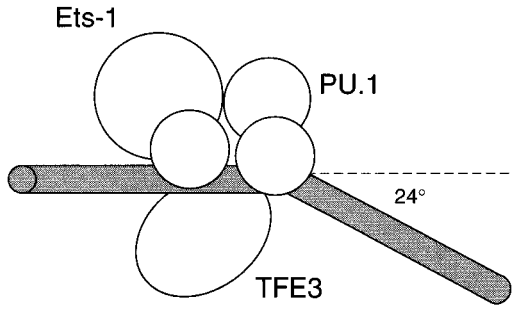

FIG. 8. Model for the functional multiprotein complex on the minimal μ enhancer. Ets-1 (μA-binding protein) and PU.1 (μB-binding protein) are shown bound to the same side of μ enhancer DNA, with the smaller circles representing the ETS domains and the larger circles representing the non-DNA-binding domains of each protein. The DNA bend of approximately 24° is shown directed away from the PU.1 protein as discussed in the text. Formation of the proposed PU.1/Ets-1 interface may be facilitated by the PU.1-induced DNA bend. The bHLH-zip protein TFE3 (μE3-binding protein) interacts with the DNA from the opposite side of the helix, with the protein located behind the plane of the paper.

In contrast to the observations of Werner et al. (59), we did not detect DNA bending by ETS(Ets-1) in circular permutation or phasing assays. One possibility for the difference in the results of the two studies is that DNA bending would be more evident with a full-length version of Ets-1. We consider this unlikely because in our assays DNA bending induced by the ETS domain of PU.1 was identical to that induced by the full-length protein. Alternatively, it is possible that the sequence of the binding site per se contributes significantly to the extent of DNA bending by Ets-1. However, for PU.1 protein, the sequence of the site appears to play a lesser role, because both the μB- and the substantially different SV40 PU.1-binding sites were bent to a similar extent upon binding this protein. Lastly, the mobility shift analysis of DNA bending may not be sufficiently sensitive to detect the small (10°) bend induced by the human Ets-1 DNA-binding domain; it is also possible that the few differences between the murine and human Ets-1 proteins further reduces the bending propensity of murine Ets-1.

It is important to note that the stereospecifically precise complex generated on μA/μB is required for enhancer activity whether the μE3 motif is being utilized (as in the case of the μ70 enhancer) or not (as in the case of the μ170 μE3$^-$ enhancer). Taken together, our data suggest that activation of the μ enhancer is driven by an ETS protein-containing nucleoprotein complex which serves as an enhancer core with the ability to utilize proximal μ enhancer elements, such as E motifs, to activate transcription.

ACKNOWLEDGMENTS

We thank Batu Erman for providing ETS (Ets-1) and the three-dimensional μ enhancer model; Kathryn Calame, Columbia University, New York, N.Y., for providing bacterial expression vectors for GST.TFE3 and GST.TFE3S; Tom Kerppola, University of Michigan, Ann Arbor, for providing the phasing vectors; A. Landy, Brown University, Providence, R.I., for providing the A tract standards; James Falvo, Harvard University, Cambridge, Mass., for assistance with phasing analysis; and Margaret Baron and Laura Cabaniss for reading the manuscript.

This work was supported by grants from the NIH (GM 38925) and the March of Dimes Birth Defects Foundation to R.S. B.N. is a recipient of a National Research Service Award (HD 07653) and an Arthritis Foundation postdoctoral fellowship. R.S. was supported by a Research Career Development Award (GM 00563) from the NIH.

REFERENCES

1. **Alessandrini, A., and S. V. Desiderio.** 1991. Coordination of immunoglobulin DJ_H transcription and D-to-J_H rearrangement by promoter-enhancer approximation. Mol. Cell. Biol. **11:**2096–2107.
2. **Bain, G., E. C. R. Maandag, D. J. Izon, D. Amsen, A. M. Kruisbeek, B. C. Weintraub, I. Krop, M. S. Schlissel, A. J. Feeney, M. van Roon, M. van der Valk, H. P. J. ter Riele, A. Berns, and C. Murre.** 1994. E2A proteins are required for proper B cell development and initiation of immunoglobulin gene rearrangements. Cell **79:**885–892.
3. **Beckmann, H., L.-K. Su, and T. Kadesch.** 1990. TFE3: A helix-loop-helix protein that activates transcription through the immunoglobulin enhancer μE3 motif. Genes Dev. **4:**167–179.
4. **Blackwell, T. K., J. Huang, A. Ma, L. Kretzner, F. W. Alt, R. N. Eisenman, and H. Weintraub.** 1993. Binding of Myc proteins to canonical and noncanonical DNA sequences. Mol. Cell. Biol. **13:**5216–5224.
5. **Blackwell, T. K., M. W. Moore, G. D. Yancopoulos, H. Suh, S. Lutzker, E. Selsing, and F. W. Alt.** 1986. Recombination between immunoglobulin variable region gene segments is enhanced by transcription. Nature (London) **324:**585–589.
6. **Bruggemann, M., J. Free, A. Diamond, J. Howard, S. Cobbold, and H. Waldmann.** 1986. Immunoglobulin heavy chain locus of the rat: striking homology to mouse antibody genes. Proc. Natl. Acad. Sci. USA **83:**6075–6079.
7. **Carr, C. S., and P. A. Sharp.** 1990. A helix-loop-helix protein related to the immunoglobulin E box-binding proteins. Mol. Cell. Biol. **10:**4384–4388.
8. **Chen, J., F. Young, A. Bottaro, V. Stewart, R. K. Smith, and F. W. Alt.** 1993. Mutations of the intronic IgH enhancer and its flanking sequences differentially affect accessibility of the J_H locus. EMBO J. **12:**4635–4645.
9. **Ephrussi, A., G. M. Church, S. Tonegawa, and W. Gilbert.** 1985. B lineage-specific interactions of an immunoglobulin enhancer with cellular factors in vivo. Science **227:**134–140.

9a. **Erman, B.** Personal communication.

10. **Fernex, C., M. Capone, and P. Ferrier.** 1995. The V(D)J recombinational and transcriptional activities of the immunoglobulin heavy-chain intronic enhancer can be mediated through distinct protein-binding sites in a transgenic substrate. Mol. Cell. Biol. **15:**3217–3226.
11. **Fisher, D. E., L. A. Parent, and P. A. Sharp.** 1992. Myc/max and other helix-loop-helix/leucine zipper proteins bend DNA toward the minor groove. Proc. Natl. Acad. Sci. USA **89:**11779–11783.
12. **Genetta, T., D. Ruezinsky, and T. Kadesch.** 1994. Displacement of an E-box-binding repressor by basic helix-loop-helix proteins: implications for B-cell specificity of the immunoglobulin heavy-chain enhancer. Mol. Cell. Biol. **14:**6153–6163.
13. **Giese, K., J. Cox, and R. Grosschedl.** 1992. The HMG domain of lymphoid enhancer factor 1 bends DNA and facilitates assembly of functional nucleoprotein structures. Cell **69:**185–195.
14. **Giese, K., C. Kingsley, J. R. Kirshner, and R. Grosschedl.** 1995. Assembly and function of a TCRα enhancer complex is dependent on LEF-1-induced DNA bending and multiple protein-protein interactions. Genes Dev. **9:**995–1008.
15. **Gilman, M. Z., R. N. Wilson, and R. A. Weinberg.** 1986. Multiple protein-binding sites in the 5′-flanking region regulate c-*fos* expression. Mol. Cell. Biol. **6:**4305–4316.
16. **Gregor, P. D., M. Sawadogo, and R. G. Roeder.** 1990. The adenovirus major late transcription factor USF is a member of the helix-loop-helix group of regulatory proteins and binds to DNA as a dimer. Genes Dev. **4:**1730–1740.
17. **Grosschedl, R., and D. Baltimore.** 1985. Cell type specificity of immunoglobulin gene expression is regulated by at least three DNA sequence elements. Cell **41:**885–897.
18. **Hagman, J., and R. Grosschedl.** 1992. An inhibitory carboxyl-terminal domain in Ets-1 and Ets-2 mediates differential binding of ETS family factors to promoter sequences of the *mb-1* gene. Proc. Natl. Acad. Sci. USA **89:**8889–8893.
19. **Hanson, R. D., J. L. Grisolano, and T. J. Ley.** 1993. Consensus AP-1 and CRE motifs upstream from the human cytotoxic serine protease B (CSP-B/CGL-1) gene synergize to activate transcription. Blood **82:**2749–2757.
20. **Hayday, A. C., S. D. Gillies, H. Saito, C. Wood, K. Wiman, W. S. Hayward, and S. Tonegawa.** 1984. Activation of a translocated human c-*myc* gene by an enhancer in the immunoglobulin heavy-chain locus. Nature (London) **307:**334–340.
21. **Hernandez-Munain, C., and M. S. Krangel.** 1994. Regulation of the T-cell receptor and enhancer by functional cooperation between c-Myb and core-binding factors. Mol. Cell. Biol. **14:**473–483.
22. **Ho, I.-C., and J. M. Leiden.** 1990. Regulation of the human T-cell receptor α gene enhancer: multiple ubiquitous and T-cell-specific nuclear proteins interact with four hypomethylated enhancer elements. Mol. Cell. Biol. **10:**4720–4727.
23. **Jenuwein, T., W. C. Forrester, R.-G. Qiu, and R. Grosschedl.** 1993. The immunoglobulin μ enhancer core establishes local factor access in nuclear chromatin independent of transcriptional stimulation. Genes Dev. **7:**2016–2032.
24. **Kadesch, T., P. Zervos, and D. Ruezinsky.** 1986. Functional analysis of the murine IgH enhancer: evidence for negative control of cell-type specificity. Nucleic Acids Res. **14:**8209–8221.
25. **Karim, F. D., L. D. Urness, C. S. Thummel, M. J. Klemsz, S. R. McKercher, A. Celada, C. VanBeveren, R. A. Maki, C. V. Gunther, J. A. Nye, and B. J. Graves.** 1990. The ETS-domain: a new DNA-binding motif that recognizes a purine-rich core DNA sequence. Genes Dev. **4:**1451–1453.
26. **Kerppola, T. K., and T. Curran.** 1991. DNA bending by fos and jun: the flexible hinge model. Science **254:**1210–1214.
27. **Kerppola, T. K., and T. Curran.** 1991. Fos-jun heterodimers and jun homodimers bend DNA in opposite orientations: implications for transcription factor cooperativity. Cell **66:**317–326.
28. **Kerppola, T. K., and T. Curran.** 1993. Selective DNA bending by a variety of bZIP proteins. Mol. Cell. Biol. **13:**5479–5489.
29. **Kim, J., C. Zwieb, C. Wu, and S. Adhya.** 1989. Bending of DNA by gene-regulatory proteins: construction and use of a DNA bending vector. Gene **85:**15–23.
30. **Lee, D.-H., and R. F. Schleif.** 1989. *In vivo* DNA loops in *ara*CBAD: size limits and helical repeat. Proc. Natl. Acad. Sci. USA **86:**476–480.
31. **Lennon, G. G., and R. P. Perry.** 1985. Cμ-containing transcripts initiate heterogeneously within the IgH enhancer region and contain a novel 5′-nontranslatable exon. Nature (London) **318:**475–478.
32. **Libermann, T. W., and D. Baltimore.** 1990. Transcriptional regulation of immunoglobulin gene expression. Mol. Aspects Cell. Regul. **6:**399–421.
33. **Lim, F., N. Kraut, J. Frampton, and T. Graf.** 1992. DNA binding by c-Ets-1, but not v-Ets, is repressed by an intramolecular mechanism. EMBO J. **11:**643–652.
34. **Lu, X. P., N. L. Eberhardt, and M. Pfahl.** 1993. DNA bending by retinoid X receptor-containing retinoid and thyroid hormone receptor complexes. Mol. Cell. Biol. **13:**6509–6519.
35. **Mage, R. G., B. A. Newman, N. Harindranath, K. E. Bernstein, R. S. Becker, and K. L. Knight.** 1989. Evolutionary conservation of splice sites in sterile Cμ transcripts and of immunoglobulin heavy chain (IgH) enhancer region sequences. Mol. Immunol. **26:**1007–1010.
36. **McBroom, L. D., G. Flock, and V. Giguère.** 1995. The nonconserved hinge region and distinct amino-terminal domains of the RORα orphan nuclear receptor isoforms are required for proper DNA bending and RORα-DNA interactions. Mol. Cell. Biol. **15:**796–808.
37. **Murre, C., P. S. McCaw, and D. Baltimore.** 1989. A new DNA binding and dimerization motif in immunoglobulin enhancer binding, daughterless, *Myo*D, and *myc* proteins. Cell **56:**777–783.
38. **Natesan, S., and M. Z. Gilman.** 1993. DNA bending and orientation-dependent function of YY1 in the c-fos promoter. Genes Dev. **7:**2497–2509.
39. **Nelsen, B., L. Hellman, and R. Sen.** 1988. The NF-κB-binding site mediates phorbol ester-inducible transcription in non-lymphoid cells. Mol. Cell. Biol. **8:**3526–3531.
40. **Nelsen, B., T. Kadesch, and R. Sen.** 1990. Complex regulation of the immunoglobulin μ heavy-chain gene enhancer: μB, a new determinant of enhancer function. Mol. Cell. Biol. **10:**3145–3154.
41. **Nelsen, B., and R. Sen.** 1992. Regulation of immunoglobulin gene transcription. Int. Rev. Cytol. **133:**121–149.
42. **Nelsen, B., G. Tian, B. Erman, J. Gregoire, R. Maki, B. Graves, and R. Sen.**

1993. Regulation of lymphoid-specific immunoglobulin μ heavy chain gene enhancer by ETS-domain proteins. Science **261:**82–86.

43. **Nye, J. A., J. Petersen, C. V. Gunther, M. D. Jonsen, and B. J. Graves.** 1992. Interaction of murine Ets-1 with GGA-binding sites establishes the ETS domain as a new DNA-binding motif. Genes Dev. **6:**975–990.
44. **Oltz, E. M., F. W. Alt, W.-C. Lin, J. Chen, G. Taccioli, S. Desiderio, and G. Rathbun.** 1993. A V(D)J recombinase-inducible B-cell line: role of transcriptional enhancer elements in directing V(D)J recombination. Mol. Cell. Biol. **13:**6223–6230.
45. **Perkins, N. D., N. L. Edwards, C. S. Duckett, A. B. Agranoff, R. M. Schmid, and G. J. Nabel.** 1993. A cooperative interaction between NF-κB and Sp1 is required for HIV-1 enhancer activation. EMBO J. **12:**3551–3558.

45a. **Rao, E., W. Dang, G. Tian, and R. Sen.** A three protein DNA complex defines a functional unit of the lymphoid-specific immunoglobulin μ heavy chain gene enhancer. Submitted for publication.

46. **Rivera, R. R., M. H. Stuiver, R. Steenbergen, and C. Murre.** 1993. Ets proteins: new factors that regulate immunoglobuin heavy-chain gene expression. Mol. Cell. Biol. **13:**7163–7169.
47. **Roman, C., L. Cohn, and K. Calame.** 1991. A dominant negative form of transcription activator mTFE3 created by differential splicing. Science **254:** 94–97.
48. **Roman, C., A. G. Matera, C. Cooper, S. Artandi, S. Blain, D. C. Ward, and K. Calame.** 1992. mTFE3, an X-linked transcriptional activator containing basic helix-loop-helix and zipper domains, utilizes the zipper to stabilize both DNA binding and multimerization. Mol. Cell. Biol. **12:**817–827.
49. **Ruezinsky, D., H. Beckmann, and T. Kadesch.** 1991. Modulation of the IgH enhancer's cell type specificity through a genetic switch. Genes Dev. **5:**29–37.
50. **Schanke, J. T., and B. G. VanNess.** 1994. The organization of the transcription factor binding sites in the κ Ig intron enhancer. J. Immunol. **153:**4565–4572.
51. **Serwe, M., and F. Sablitzky.** 1993. V(D)J recombination in B cells is impaired but not blocked by targeted deletion of the immunoglobulin heavy chain intron enhancer. EMBO J. **12:**2321–2327.
52. **Shen, L., S. Lieberman, and L. A. Eckhardt.** 1993. The octamer/μE4 region of the immunoglobulin heavy-chain enhancer mediates gene repression in myeloma X T-lymphoma hybrids. Mol. Cell. Biol. **13:**3530–3540.
53. **Smith, D. B., and K. S. Johnson.** 1988. Single-step purification of polypeptides expressed in *Escherichia coli* as fusions with glutathione S-transferase. Gene **67:**31–40.
54. **Sun, S.-H.** 1994. Constitutive expression of the *Id1* gene impairs mouse B cell development. Cell **79:**893–900.
55. **Takahashi, K., M. Vigneron, H. Mattes, A. Wildeman, M. Zenke, and P. Chambon.** 1986. Requirement of stereospecific alignments for initiation from the simian virus 40 early promoter. Nature (London) **319:**121–126.
56. **Thompson, J. F., and A. Landy.** 1988. Empirical estimation of protein-induced DNA bending angles: applications to λ site-specific recombination complexes. Nucleic Acids Res. **16:**9687–9705.
57. **Vilen, B. J., J. P. Cogswell, and J. P. Ting.** 1991. Stereospecific alignment of the X and Y elements is required for major histocompatibility complex class II DRA promoter function. Mol. Cell. Biol. **11:**2406–2415.
58. **Wasylyk, C., J.-P. Kerckaert, and B. Wasylyk.** 1992. A novel modulator domain of Ets transcription factors. Genes Dev. **6:**965–974.
59. **Werner, M. H., G. M. Clore, C. L. Fisher, R. J. Fisher, L. Trinh, J. Shiloach, and A. M. Gronenborn.** 1995. The solution structure of the human ETS1-DNA complex reveals a novel mode of binding and true side chain intercalation. Cell **83:**761–771.
60. **Wooton, D., J. Ghysdael, S. Wang, N. A. Speck, and M. J. Owen.** 1994. Cooperative binding of Ets-1 and core binding factor to DNA. Mol. Cell. Biol. **14:**840–850.
61. **Zhuang, Y., P. Soriano, and H. Weintraub.** 1994. The helix-loop-helix gene E2A is required for B cell formation. Cell **79:**875–884.
62. **Zinkel, S. S., and D. M. Crothers.** 1991. Catabolite activator protein-induced DNA bending in transcription initiation. J. Mol. Biol. **219:**201–215.